Vortex motion at high frequencies in superconductors: insights into microwave power dependence

James C. Booth, Dong Ho Wu, and Steven M. Anlage

Maryland Center for Superconductivity Research, Physics Department, University of Maryland, College Park, Maryland 20742-4111 USA

ABSTRACT

We present a brief description of the role played by the motion of magnetic vortices in the power dependence and non-linearity of high T_c superconductors at rf and microwave frequencies. We then review the current understanding of vortex motion at rf and microwave frequencies, and present broadband (45 MHz - 50 GHz) experimental results which shows a striking crossover in the behavior of the vortex dynamics from a low-frequency interaction-dominated regime, to a high frequency essentially single-particle regime. Finally, we discuss the impact these different regimes of vortex motion have on the design and operation of high T_c rf and microwave devices.

Keywords: superconductivity, microwave, vortex motion, power dependence

1. INTRODUCTION

The most promising near-term significant application of high T_c superconductivity is in rf and microwave subsystems and components. Many of these applications require superconducting devices to operate under non-optimum conditions, such as large magnetic fields and/or high microwave power. Under such conditions, where high microwave power may induce an rf critical state,[1] the most significant limitations to the widespread use of high T_c components are the considerable power dependence exhibited by both passive and active devices, and higher-order harmonic generation caused by non-linearities in the surface impedance. Many of these limitations are directly related to the generation and/or motion of magnetic vortices under the influence of rf or microwave fields.

The importance of understanding vortex motion at microwave frequencies results from a simple consequence: vortex motion in a superconductor causes loss. In addition, at finite frequencies the presence of vortices will influence the surface impedance, causing non-linearities which can give rise to unwanted harmonic generation and mode conversion. The frequency range from 45 MHz to 50 GHz includes many technologically important applications, such as cellular telephone, PCS, and radar systems, and many devices that operate at these frequencies will need to explicitly take into account the effects of vortex motion if they are expected to operate at high powers or fields. Also, such information is essential for non-reciprocal devices such as circulators and isolators that require a fixed magnetic field to operate.[2]

This paper will examine the effect of the driving frequency on vortex motion in thin-film superconductors in this high-field/high-power regime, with the ultimate goal of understanding the source of the power dependence and non-linearity of present and future high T_c microwave devices. We will not address the issue of how vortices enter the film, but will focus instead on the response of high T_c thin films when magnetic vortices are present. We find that the response of the superconductor depends sensitively on the driving frequency, with a given response at low frequencies ($\leq$ 1 GHz), and a very different response for high frequencies ($\geq$ 10 GHz) for many temperatures and magnetic field strengths.

2. VORTEX MOTION AT RF AND MICROWAVE FREQUENCIES

Here we will attempt to describe how one understands vortex motion in superconductors at rf and microwave frequencies. We will simplify the discussion by examining separately the low frequency and high frequency limits in the context of various theoretical models, and then will address what happens experimentally in these two regimes, as well as in the intermediate frequency region.

0-8194-1918-4/95/$6.00

In the conventional superconductors, one understands the low frequency ac response in terms of the same mean-field phase diagram that one uses at dc. At fields and temperatures above $H_{c1}(T)$ one enters the mixed state, characterized by a rigid Abrikosov vortex lattice that persists until the upper critical field, $H_{c2}(T)$, is exceeded. The response in the mixed state at finite frequencies is governed by the strength of the pinning in the material, with "superconducting" behavior observed as long as the ac current density is less than the dc critical current value. In the high frequency limit, however, one can observe drastically different behavior:[3] the sudden onset of loss occurs in the superconductor as one passes a characteristic frequency (called the "depinning frequency"), even with subcritical ac current densities. Above this frequency the entire vortex lattice oscillates in phase with the driving frequency, giving the same response as one would observe in the absence of any pinning. Hence for conventional superconductors in the mixed state, one can clearly demarcate two distinct regions in frequency: a low-frequency, lossless regime in which the vortex lattice is effectively pinned ($f < f_{depin}$), and a high-frequency, lossy regime ($f > f_{depin}$) in which the response of the vortex lattice is the same as if the pinning were absent and the vortices were free to move. For the conventional superconductor PbIn, the "depinning frequency" is on the order of ~7 MHz at 1.7 K, while for NbTa at 4.2 K the value is ~26 MHz.[3]

In the high T_c superconductors a number of factors, such as the short coherence lengths, strong anisotropy, and large thermal energies conspire to make the situation in the mixed state more complicated. In the low frequency limit the main effects on the mixed state are the following: (a) the vortex lattice state is replaced by a novel vortex glass state, in which the long range crystalline order of the vortex lattice is destroyed by pinning disorder and thermal fluctuations, and (b) the appearance of a "vortex liquid" state at fields and temperatures well below the upper critical field $H_{c2}(T)$. Fig. 1 shows a possible phase diagram for the high T_c superconductor $YBa_2Cu_3O_{7-\delta}$ (YBCO).[4] The vortex glass state remains a "true superconducting" state in which the losses go to zero in the limit of very small current. For large currents, however, the current-voltage response in the vortex glass state can become very non-linear. The vortex liquid state is characterized by finite losses in the superconductor for arbitrarily small currents. This means that any practical device that makes use of superconducting properties must be operated well below the vortex "melting" transition $H_m(T)$.[5]

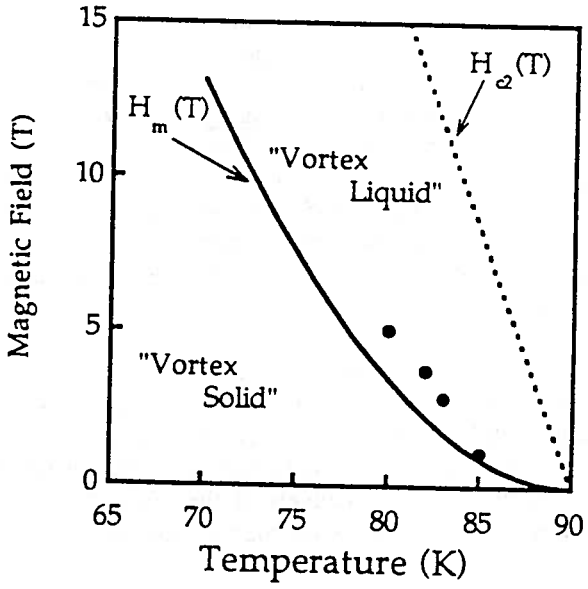

Fig. 1. Possible vortex phase diagram for YBCO. The "melting" line $H_m(T)$ separates a vortex solid state from a vortex liquid state. The data points represent an experimental determination of the phase boundary as discussed in section 4.

The existence of a vortex glass state and the associated glass to liquid transition has been predicted by Fisher, Fisher, and Huse.[6] Experimental evidence for such a transition has been observed in dc measurements[7] and

in finite frequency measurements[8,9] on YBCO thin films. The finite frequency measurements show that at the liquid to glass transition the frequency dependence of the real and imaginary parts of the complex resistivity can be written as power laws:

$$\rho_1(\omega) \sim \omega^{\alpha_1} \qquad \rho_2(\omega) \sim \omega^{\alpha_2}$$

with $\alpha_1 = \alpha_2$ ($\cong 0.73$) at the vortex liquid to glass transition[9], and with $\alpha_1 > (<)\ \alpha_2$ below (above) the glass to liquid transition. The ac measurements described above did not extend into the microwave regime, with the highest measured frequency being approximately 600 MHz. It should be pointed out that in the conventional superconductors this "melting" transition occurs essentially at the upper critical field $H_{c2}(T)$ and the vortex liquid region in the H-T phase diagram is unobservably narrow.

For the high T_c superconductors one might also expect qualitatively different behavior if the driving frequency is sufficiently high. This is because as the measurement frequency increases, the probing time scale becomes shorter, not allowing vortex lines enough time to interact with other vortices. Hence for high frequencies one might expect mean field models such as those employed for conventional superconductors to be more appropriate than the vortex interaction based glass/liquid models mentioned above. In this limit the vortices behave as individual flux lines. However, the short coherence length and random pinning potential in the high T_c superconductors mean that the interaction between the pinning potential and the vortices may be more complicated than for the conventional superconductors, where it is assumed that the rigid vortex lattice interacts with a single periodic pinning potential.

Several experiments performed on YBCO films at microwave frequencies (~10 GHz)[10-12] have been successfully interpreted using mean-field based models.[13] Measurements in the terahertz regime[14] (500 GHz-1 THz) also support the mean-field picture. In addition, far infrared measurements[15] are also in agreement with single-particle models[16] that neglect vortex-vortex interactions. The value of the "depinning frequency" for YBCO extracted from the microwave measurements[10-12] seems to be much higher than for the conventional materials (~40 GHz at 77 K[11]), which would imply a much wider operational frequency range for a high T_c device at a given temperature. However, these results seem to be in contradiction with the lower frequency experiments that support the vortex glass-based models described above.

3. EXPERIMENT: CORBINO MEASUREMENTS

Given the above considerations, measurements on superconductors spanning a wide frequency range in the rf, microwave, and millimeter-wave regimes seem very desirable. Fig. 2 shows the experiment setup of such a measurement,[17] in which the superconducting film forms a short circuit across a coaxial transmission line. The complex reflection coefficient S_{11} is then measured over the continuous frequency range from 45 MHz to 50 GHz using an HP8510C vector network analyzer. The measured reflection coefficient S_{11} is related to the surface impedance Z_s of the film by the relation

$$Z_s(T,B,\omega) = Z_0 \frac{1 + S_{11}(T,B,\omega)}{1 - S_{11}(T,B,\omega)}$$

where Z_0 is the characteristic impedance of the TEM mode in the coaxial line. For a film of thickness $t_0 << \lambda$ (where λ is the penetration depth of the film), the measured surface impedance can be simply related to the complex resistivity ρ^* ($= \rho_1 + i\rho_2$) by

$$Z_s(T,B,\omega) = \frac{\rho^*(T,B,\omega)}{t_0} \qquad (t_0 << \lambda)$$

Hence by measuring the complex reflection coefficient of a superconducting film as a function of frequency, temperature, and external magnetic field strength, we are able to obtain simply the complex resistivity over this wide parameter space. Note also from Fig. 2 that the superconductor can be biased with a dc current and that the dc resistance can be measured simultaneously with the ac measurement.

Such an experimental configuration offers several advantages. The disk-shaped region of the sample exposed between the inner and outer coaxial conductors is referred to as the Corbino geometry, and is beneficial

when studying vortex motion because the edges of the sample are effectively eliminated and do not contribute to the creation and/or pinning of vortices. The coaxial geometry also means that the same mode (TEM) can be used to measure at all frequencies, as opposed to stripline or microstrip resonators, which use different modes, and hence different field distributions, for different (discrete) frequencies. Another result of using the coaxial TEM mode is that the field distribution in the film is particularly simple, with the fields and currents proportional to 1/r, and uniform throughout the film thickness (for sufficiently thin films).

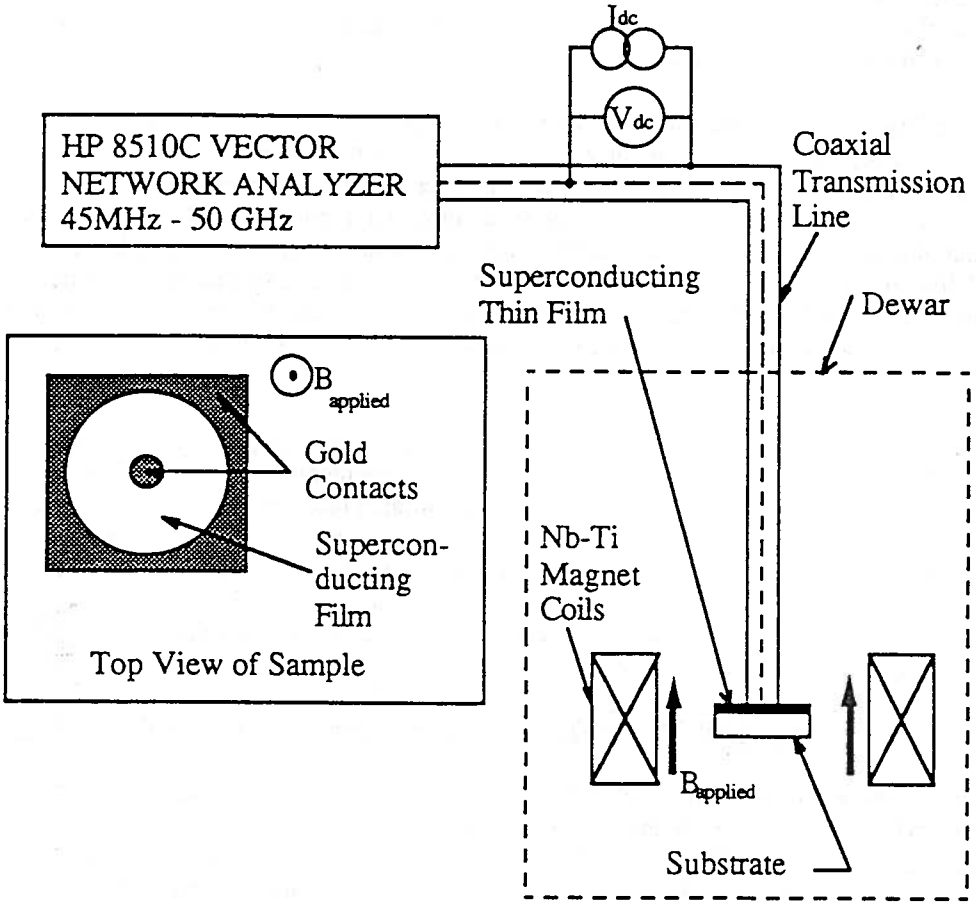

Fig. 2. Schematic diagram of reflection measurement apparatus. The coaxial cable can also be biased with an external dc current. The inset shows a top view of the Corbino contact to the superconducting film.

The experimental technique described above can be used to measure the response of the superconducting mixed state over a very wide and technologically important frequency range (45 MHz - 50 GHz) in the rf and microwave regime. The sensitivity allows for measurement of changes in the complex resistivity ρ^* of $\sim 10^{-9}$ Ωm at low frequencies for a 1000 Å film. Also, for a perfectly conducting standard, the system measures a reflection coefficient of magnitude unity to ±4% over the entire frequency range. The ac current density can also be varied, by changing the microwave power, although for the measurements described here it was kept small, approximately 80-200 A/cm^2. Experiments were carried out with several c-axis YBCO thin films of thickness ~1000Å fabricated by pulsed laser deposition on $LaAlO_3$ substrates.

4. EXPERIMENTAL RESULTS

Data from our measurements of the mixed state of YBCO thin films is shown in Figs. 3 and 4, which display the frequency dependence of the real and imaginary parts respectively of the complex resistivity at a temperature of 80.2 K and an applied magnetic field of 0.4 T. The complex resistivity ρ^* relates the time dependent electric field to the time dependent current density in the superconductor according to

$$E = \rho^* J$$

The real part of the complex resistivity ρ_1 is a measure of the energy loss, while the imaginary part ρ_2 is a measure of the reactance, or energy stored. Also shown Fig. 3 are mean-field fits to the data (dashed lines), and fits to the vortex solid to liquid scaling forms $\rho_1 \sim \omega^{\alpha}1$ and $\rho_2 \sim \omega^{\alpha}2$ (solid lines). The fitting function for the mean field fits is taken from ref. 13 and is given by

$$\rho^*(\omega) = \rho_f \frac{\varepsilon + (\omega\tau)^2 + i\,(1-\varepsilon)\,\omega\tau}{1 + (\omega\tau)^2}$$

where ρ_f is the flux-flow resistivity, which is the loss one would measure due to vortex motion with no pinning: $\rho_f = B\phi_0/\eta$, where η is the vortex viscosity coefficient, B is the applied magnetic field, and ϕ_0 is the flux quantum. Also, ε is the flux-creep factor (which is bounded between 0 and 1) and τ is the plucked vortex relaxation time.

Figs. 3 and 4 clearly show one of the major results of our work: at low frequencies the data follow the vortex solid to liquid scaling models, while at high frequencies the data show good agreement with a mean field description. Measurements carried out at other points in the B-T phase space near the liquid to glass transition show similar behavior. The cross-over frequency from scaling to mean-field behavior occurs for the data in Figs. 3 and 4 at about 10 GHz, and the data shows a smooth transition from the low-ω regime to the high-ω regime. We can obtain the characteristic vortex relaxation time τ (which gives the "depinning frequency" $f_{depin} \sim 1/\tau$) from the mean-field fit to the high frequency data. We find for instance at T=78 K and H=0.3 T, that $1/\tau \sim 13 \times 10^9$ sec^{-1}, which is somewhat larger than earlier results from YBCO crystals,[18] but smaller than that obtained for a thick (~1μm) YBCO film.[11] Also, using the value of ρ_f obtained from the fit, we extract $\eta \sim 2 \times 10^{-8}$ Nsec/m^2 for T=80.2 K and H_{dc} = 0.4 T. The mean-field fits also give values of ε in the range $0.05 < \varepsilon \leq 0.5$ for 80 K < T < 86 K and $0 < H_{dc} < 1$ T.

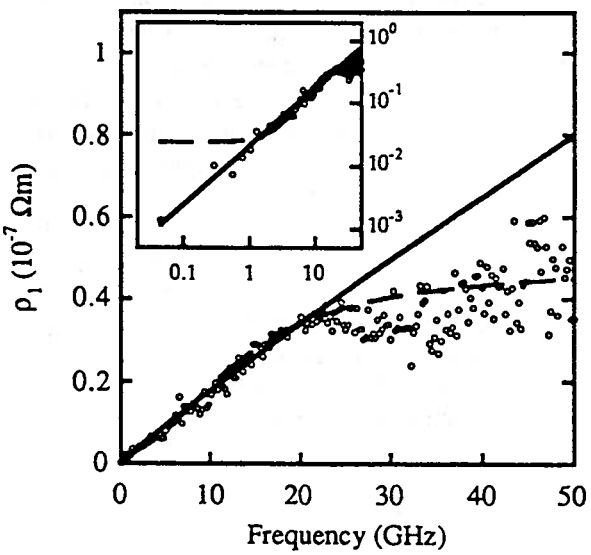

Fig. 3. The frequency dependence of $\rho_1(\omega)$ for a YBCO c-axis thin film at T=80.2 K and H=0.4 T. The solid line represents $\rho_1 \propto \omega^{\alpha}1$, with $\alpha_1 = 0.81$, and the dashed line represents the mean-field fit. The inset shows the same data on a log-log plot.

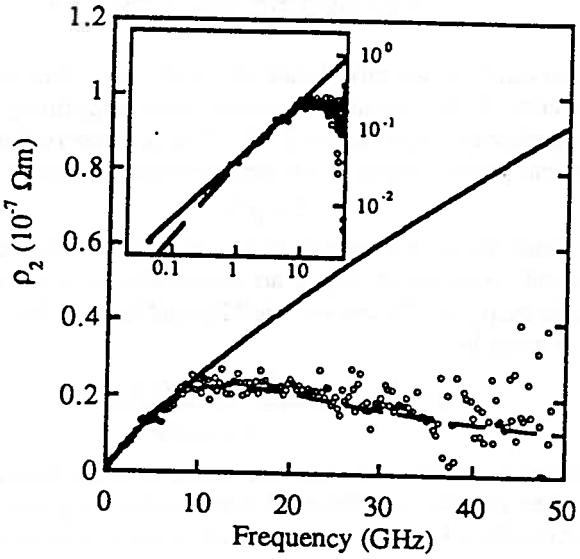

Fig. 4. The frequency dependence of $\rho_2(\omega)$ for a YBCO c-axis thin film at T=80.2 K and H=0.4 T. The solid line represents $\rho_2 \alpha \omega^{\alpha}2$, with $\alpha_2 = 0.93$, and the dashed line represents the mean-field fit. The inset shows the same data on a log-log plot.

We can also gain some insight into the nature of vortex motion from the detailed shape of the ρ_1 vs. H_{dc} curves shown in Fig. 5, which displays $\rho_1(H)$ measured at T=83.5 K for various frequencies, along with mean-field fits. The mean-field fits are obtained using the full expressions for ρ^* (given above) and $\tau = \eta/\kappa_p[\{I_0^2(\nu) - 1\}/\{I_1(\nu)\, I_0(\nu)\}]$ with variables $\nu = U_0(H)/2k_BT$ and $\varepsilon = I_0(\nu)^2$, where $I_0(\nu)$ and $I_1(\nu)$ are modified Bessel functions of the first and second kind, which account for the thermally activated hopping of vortices over barriers of height U_0. Note that ν can be written as $\nu = H^*/H$ if we assume the barrier height depends on the magnetic field as $U_0 \sim 1/H$, so that $H = H^*$ represents the field at which $U_0(H) = 2k_BT$ and significant flux creep begins to occur. The data measured at 11 and 13 GHz follow the mean-field description for all fields. The 11 and 13 GHz fits yield values for $H^* \sim 3.5$ Tesla, $\eta \sim 3.2 \times 10^{-8}$ Nsec/m^2 and a pinning force constant $\kappa_p = 3.5\text{-}4.5 \times 10^3$ N/m^2. The low frequency data (f=3 GHz and 6 GHz), however, cannot be reconciled with the mean-field fit with reasonable parameter values. The magnetic field dependence therefore corroborates the conclusion drawn from the frequency dependent data: the mean-field description is adequate for the high frequency data ($f \geq 10$ GHz) while the low frequency data requires consideration of vortex-vortex interactions.

The ρ_1 vs. H curves for the high frequency data can also be used to locate approximately the "melting transition" in the H-T phase diagram. If we take as a criterion for melting that $\rho_1(H_m) \approx 0.1\rho_n$, where ρ_n is the normal state resistivity at T_c, then one obtains for the "melting line" the points shown in Fig. 1. The field for which this criterion is satisfied also corresponds to a peak in the quantity $\rho_2(H)/H$ vs. H, which is the imaginary part of the dynamic mobility of the vortex in the mean field picture[13] ($\rho^* = B\phi_0\mu^*$, where μ^* is the complex dynamic mobility). Although this is not a stringent criterion for the melting of the vortex lattice,[5] it provides an order of magnitude estimate for $H_m(T)$.

5. DISCUSSION

Our experimental results serve to connect two seemingly contradictory sets of experimental results. The dc and low frequency experiments show much evidence for the existence of a vortex glass/liquid state. However, microwave, THz, and far-infrared experimental results are well described by the mean-field models. Our experiments show that both sets of results are in fact consistent, with the broad frequency range of our measurements providing a bridge between these two very different regimes. The crossover from the vortex glass/liquid scaling behavior to the

mean-field-like behavior as the frequency increases is likely related to a crossover from *intervalley transitions*,[19] where the vortices move collectively by thermally activated hops between different metastable states in the random pinning potential, to *intravalley oscillations*,[19] where the vortices move individually and the motion is dominantly confined within the random pinning potential well. Here we will consider the implications of such a picture for practical devices expected to operate at rf and microwave frequencies.

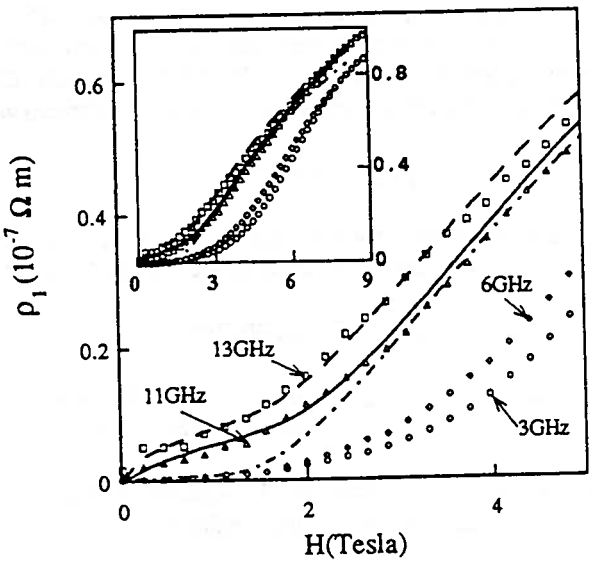

Fig. 5. Field dependence of $\rho_1(H)$ for a YBCO thin film for various frequencies at T=83.5 K. Dashed-dot line is a mean field fit for 3 GHz. Solid line and dashed line are mean field fits for 11 and 13 GHz respectively. Inset: $\rho_1(H)$ for $0 \le H \le 9$ T.

The lack of a theory for the finite frequency response of both the vortex glass and vortex liquid states away from the glass-to-liquid transition makes it difficult to accurately predict the response of a device operated in these regions of phase space. Our results indicate that one must go to high frequencies (> 10 GHz for the temperatures and field strengths investigated here) before the details of the pinning potential and vortex viscosity become important. It is therefore necessary to further study the ac response, particularly of the vortex glass state, to better predict the behavior of a practical device operated in this (large) region of the B-T phase diagram.

Note that the scaling theory predicts the behavior of $\rho(\omega)$ at the vortex glass-to-liquid transition will be universal, independent of the microscopic details of the system, so that there is little one can do experimentally to engineer the vortex behavior at the glass-to-liquid transition. However, if one wants highly reproducible surface impedance properties in a magnetic field, the vortex glass-to-liquid transition is very attractive. To take advantage of this, one can design a non-reciprocal device to operate at a magnetic field strength and temperature which is near, but just below, the vortex glass-to-liquid transition.

The complicated mixed state response of the high T_c superconductors has many other consequences for applications. The existence of a "melting" transition well below the upper critical field imposes additional design constraints for high T_c devices. To fully exploit the advantages offered by superconducting materials, such devices should be operated below the "melting" line $H_m(T)$ shown in Fig. 1. Therefore, for both dc and rf/microwave devices, it is important to maximize the pinning strength of the material, in order to push the melting line $H_m(T)$ to the highest possible fields and temperatures.

The existence of a "depinning frequency" implys a maximum operable frequency for an ac device at a given field and temperature. The mean-field expression[13] for $f_{depin} = 1/\tau \sim \kappa_p/\eta$ shows that increasing the strength of the

pinning also helps to increase the "depinning frequency." Above this frequency the pinning strength of the material becomes less and less important, and materials controls lose their effectiveness.

6. CONCLUSIONS

In summary, understanding the behavior of vortices in high T_c superconductors at rf and microwave frequencies is necessary for the development and operation of many practical high T_c devices. To that end, we have shown experimental evidence for a crossover in the frequency response of the mixed state of the high T_c superconductor YBCO from a low-frequency regime that can be described by vortex glass/liquid models to a high frequency regime which can be well described by mean-field models. Such experimental results provide important insights into the power dependence and non-linearities of high T_c microwave and rf devices, which helps to remove these barriers to the more widespread application of superconductivity at rf and microwave frequencies.

7. ACKNOWLEDGEMENTS

We thank C. J. Lobb and R. L. Greene for stimulating discussions and A. Findikoglu and C. Kwon for assistance with sample preparation. This work was supported by the NSF NYI program DMR-9258183.

8. REFERENCES

[1]C. C. Chin, D. E. Oates, G. Dresselhaus, M. S. Dresselhaus, "Nonlinear electrodynamics of superconducting NbN and Nb thin films at microwave frequencies," Phys. Rev. B 45, pp. 4788-4798 (1992).

[2]A. Fathy, E. Denlinger, D. Kalokitis, V. Pendrick, H. Johnson, A. Pique, K. S. Harshavardhan, E. Belohoubek, "Miniature Circulators for Microwave Superconducting Systems," 1995 IEEE MTT-S Symposium Digest vol. 1, pp.195-198 (1995).

[3]J. I. Gittleman and B. Rosenblum, "The Pinning Potential and High-Frequency Studies of Type-II Superconductors," J. Appl. Phys. 39, pp. 2617-2621 (1968).

[4]The upper critical field is approximated as $H_{c2}(T) = 1.65(T_c-T)$, while the melting line is approximated by $H_m(T) = [T_c (-dH_{c2}/dT)] A [1-T/T_c]^2/\{1 + [1+B (1-T/T_c)]^{1/2}\}^2$, with A=8 and B = 1, and H_{c2} given above, and with T_c = 90 K (see reference 5).

[5]For a much more thorough discussion of melting and the vortex liquid-to-solid transformation, see D. E. Farrell in *Physical Properties of High Temperature Superconductors IV*, D. M. Ginsberg, Ed., (World Scientific, Singapore,1994), pp. 7-59.

[6]D. S. Fisher, M. P. A. Fisher, D. A. Huse, "Thermal fluctuations, quenched disorder, phase transitions, and transport in type-II superconductors," Phys. Rev. B 43, pp. 130-159 (1992).

[7]R. H. Koch, V. Foglietti, W. J. Gallagher, G. Koren, A. Gupta, and M. P. A. Fisher, "Experimental Evidence for Vortex-Glass Superconductivity in Y-Ba-Cu-O," Phys. Rev. Lett. 63, pp. 1511-1514 (1989).

[8]H. K. Olsson, R. H. Koch, W. Eidelloth, and R. P. Robertazzi, "Observation of Critical Scaling Behavior in the ac Impedance at the Onset of Superconductivity in a Large Magnetic Field," Phys. Rev. Lett. 66, pp. 2661-2664 (1991).

[9]H. Wu, N. P. Ong, and Y. Q. Li, "Frequency Dependence of the Vortex-State Resistivity in $YBa_2Cu_3O_{7-\delta}$," Phys. Rev. Lett. 71, pp. 2462-2465 (1993).

[10]J. Owliaei, S. Sridhar, and J. Talvacchio, "Field-Dependent Crossover in the Vortex Response at Microwave Frequencies in $YBa_2Cu_3O_{7-\delta}$ Films," Phys. Rev. Lett. 69, pp.3366-3369, (1992).

[11]M. S. Pambianchi, D. H. Wu, L. Ganapathi, and S. M. Anlage, "DC Magnetic Field Dependence of the Surface Impedance in Superconducting Parallel Plate Transmission Line Resonators", IEEE Trans. Appl. Supercond. 3, pp. 2774-2777, (1993).

[12]M. Golosovsky, M. Tsindlekht, H. Chayet, and D. Davidov, "Vortex depinning frequency in $YBa_2Cu_3O_{7-x}$ superconducting thin films - anisotopy and temperature dependence," Phys. Rev. B 50, pp. 470-477, (1994).

[13]M. W. Coffey and J. R. Clem, "Unified Theory of Effects of Vortex Pinning and Flux Creep upon the rf Surface Impedance of Type-II Superconductors," Phys. Rev. Lett. 67, pp. 386-389 (1991).

[14]B. Parks, S. Spielman, J. Orenstein, D. T. Nemeth, F. Ludwig, J. Clarke, P. Merchant, D. J. Lew, "Phase-sensitive measurements of vortex dynamics in the terahertz domain," Phys. Rev. Lett. 74, pp. 3265-3268 (1995).

[15]E.-J. Choi, H.-T. S. Lihn, H. D. Drew, and T. C. Hsu, "Magneto-optics of type-II superconductors," Phys. Rev. B 49, pp. 13271-13274.

[16]T. C. Hsu, "Frequency dependent conductivity of vortex cores in type II superconductors," Physica C 213, pp. 305-320 (1993).

[17]J. C. Booth, D. H. Wu, and S. M. Anlage, "A broadband method for the measurement of the surface impedance of thin films at microwave frequencies," Rev. Sci. Instrum. 65, pp. 2082-2090 (1994).

[18]D. H. Wu and S.Sridhar, "Pinning Forces and Lower Critical Fields in $YBa_2Cu_3O_y$ Crystals: Temperature Dependence and Anisotropy,", Phys. Rev. Lett. 65, pp. 2074-2077 (1990).

[19]V. B. Geshkenbein, V. M. Vinokur, R. Fehrenbacher, "ac absorption in the high-T_c superconductors: Reinterpretation of the irrevervsibility line," Phys. Rev. B 43, pp. 3748-3751 (1991).